ACS Sustainable Chemistry & Engineering

Research Article

pubs.acs.org/journal/ascecg

Microwave-Assisted Recycling of Waste Paper to Green Platform Chemicals and Carbon Nanospheres

Salman Hassanzadeh, Nina Aminlashgari, and Minna Hakkarainen*

Department of Fibre and Polymer Technology, KTH Royal Institute of Technology, Teknikringen 58, SE-100 44 Stockholm, Sweden

Supporting Information

ABSTRACT: Effective high-yield recycling of waste paper to well-defined future platform chemicals and carbon nanospheres was demonstrated. The developed process utilized the exceptional combined effect of microwave irradiation and dilute acid catalyst to hydrothermally degrade cellulose in waste paper. The process was evaluated for three different waste papers, brown and white paper tissues and white printing paper. Different pretreatment processes were investigated to further increase the cellulose liquefaction efficiency. By utilizing soda pretreatment, liquefaction efficiencies as high as 88% were achieved. The obtained liquefaction products were fingerprinted by NMR and LDI-MS, while the solid residues were analyzed by XRD, SEM, TGA, and FTIR. As industrial-scale microwave reactors are currently under development, the developed method displays significant potential for recycling waste paper to green platform chemicals at the industrial scale.

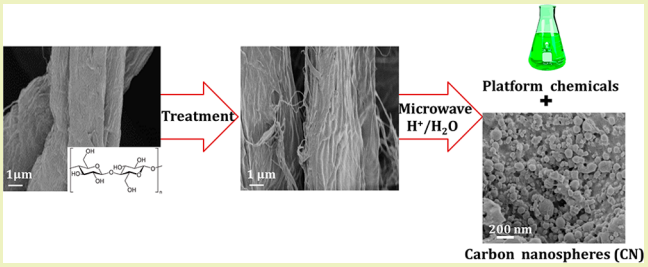

KEYWORDS: *Microwave recycling, Waste paper, Cellulose, Hydrothermal degradation, Liquefaction, Carbon nanospheres*

INTRODUCTION

The recent concerns on shrinking unrenewable oil resources and related environmental problems have raised new policies regarding the use of sustainable resources for fuel and chemical production.[1,2] Sustainable development also demands taking care of the waste produced and finding new ways to recycle waste to value-added products. For example, at the moment, waste paper corresponds to more than 40% of the whole United States trash, equaling more than 71 million tons per year.[3] The environmental risk of managing downgraded waste paper (waste paper fibers that have been recycled several times) such as landfilling incineration is high.[4,5] At the same time, valuable raw material is disregarded as these low quality paper products could be new cheap cellulosic resources for production of new platform chemicals and materials.

Cellulose, the main raw material for production of paper, is the most abundant organic compound on Earth. It is the main structural component of the primary cell wall of green plants and can be produced also by algae, oomycetes, and some bacteria. It is also one of the main bioresources not competing with food production.[6,7] On the basis of the report by the Food and Agriculture Organization of the United Nations (FAO),[8] *"Successful utilization of cellulosic materials as renewable carbon sources is dependent on the development of economically feasible process technologies for cellulose production, and for the enzymatic hydrolysis of cellulosic materials to low molecular weight products such as hexoses and pentoses"*. They also emphasize that cellulose production is the most expensive step during ethanol production from cellulosic biomass corresponding to 40% of the total cost. Therefore, significant reduction in the cellulose starting material cost is a key step for commercial viability of cellulose production technology. Another report from United Nations Environment Programme[9] states that improper management of agricultural and cellulosic biomasses including waste paper can produce more methane, contaminate leachate, and finally generate more CO_2. A suitable recycling and biorefinery plan for waste paper after it can no longer be recycled to new paper products is, thus, of utmost importance.

The physicochemical behavior and resistance of native cellulose for hydrothermal hydrolysis reaction is influenced mainly by its protected β (1−4)-glycosidic linkages within crystalline (I) structure and interchain, intrachain, and intersheet networks of hydrogen bonding.[10−13] An efficient process for hydrothermal degradation of cellulose requires first decreasing the order of the cellulose chains through disruption of the hydrogen bonds and second efficient hydrolysis of the glycosidic linkages. In this regard, different pretreatments have been employed to disrupt the hydrolysis prohibiting interactions, to increase pulping, to change cellulose crystallinity and polymerization degree, to increase surface area, porosity, catalysis access, and swelling of the material, and to purify biomass waste from additives.[14−20] All these parameters are favorable for increasing the hydrolysis rate and for facilitating the nucleophilic attack of the glycosidic bond.[21]

Microwave-assisted reactions have created revolutionary developments in organic synthesis, and microwave-assisted processes are also emerging as viable technologies for chemical recycling of polymers and biomass.[22−33] In addition, microwave-assisted

Received: November 1, 2014
Revised: December 1, 2014
Published: December 10, 2014

reactions are generally greener and relatively easy to scale up.[34,35] The potential of the microwave-assisted reaction to effectively decrystallize, dissolute, and depolymerize cellulose at relatively low temperatures and under mild reaction conditions was recently confirmed.[36−38] In addition, it was shown that the reaction leads to chemo-selective production of a few well-defined platform chemicals. We hypothesized that a similar reaction could effectively turn waste paper into value-added chemicals including glucose (Glc), hydroxymethylfurfural (HMF), levulinic acid (LeA), and formic acid (FA) as well as carbonous structures. While levulinic acid, glucose, and formic acid display great potential as future platform chemicals from biorefinaries,[39] carbon nanospheres are promising materials for versatile applications ranging from lithium batteries[40] to therapeutic devices.[41] To further facilitate the hydrothermal degradation of waste paper, different simple low cost industrially applicable pretreatment methods were also evaluated.

EXPERIMENTAL SECTION

Materials. Cellulose-rich waste products including brown paper tissues (BT) (KATRIN Basic (25 cm × 20.6 cm) hand towel M2, Metsä Tissue Corporation), white paper tissues (WT) (KIMTECH science tissue wipers (21 cm × 20 cm) Kimberly-Clark professional Company), white printing paper (WP) (copy paper A4 (21 cm × 29.7 cm) 80g/m^2 XEROX Company), and pure α-cellulose from Sigma-Aldrich as a reference material were included in the study. α-Cellulose was dried in vacuum oven overnight (25 °C) before use. Sulfuric acid (SA) (95−98%) and sodium hydroxide (>98%) were purchased from Sigma-Aldrich and were used as received. Deuterium oxide was obtained from Cambridge Laboratories (99.9%). Deionized water was used for preparation of all the aqueous reaction solutions.

Instruments and Methods. *Pretreatment of Paper Waste.* Prior to the microwave reaction, different pretreatments of waste paper were evaluated to enhance pulping, surface area, and cellulose swelling, to purify the paper materials from additives, and to potentially decrease the degree of polymerization and crystallinity (by soda pretreatment). The simplicity and industrial favorability were considered when choosing the pretreatment methods. The selected pretreatment methods included water swelling, acid wetting, soda treatment, and sonication.

(1). Water Swelling. The shredded waste paper samples (0.5 g) were soaked and stirred (magnetic stirring, 150 rpm) for 24 h in 20 mL water before the main microwave reaction. The desired concentration of sulfuric acid was added to the solution before the microwave reaction.

(2). Acid Wetting. The shredded waste paper samples (0.5 g) were soaked in 20 mL acidic solution (0.01 g/mL H_2SO_4 solution) and stirred for 30 min (magnetic stirring, 150 rpm) at room temperature. Moderate time and temperature were chosen to avoid depolymerization before running the main microwave reaction.

(3). Sonication. To take the advantage of mechanical shear force, the shredded waste paper samples (0.5 g) were soaked in 20 mL acidic solution and sonicated for 30 min at 45 °C at sonication bath (Bransonic Ultrasonic cleaners, model 2210, 40 kHz, 130 W) before the microwave reaction.

(4). Soda Pretreatment. On the basis of the procedure suggested by Obumneme as optimum soda pulping condition for cellulosic biomasses,[42] 4 g of shredded waste paper was added to 50 mL of aqueous solution containing 5 wt % NaOH (pH ∼ 14). Vigorous agitation (magnetic stirring, 400 rpm) was applied for 180 min at 55 °C. The final product was filtered and washed continuously with deionized water to reach neutral pH before drying in the vacuum oven for 24 h at 25 °C.

Microwave Reactions. The microwave reactions were run in sulfuric acid solution (0.01 g/mL, pH ∼ 1) in a MES-1000 (CEM Corporation) microwave with a maximum power of 950 W ± 50. The experiments were performed on dynamic mode where the microwave reactor will reach and keep the desired temperature by input of irradiation. The microwave was operated with full power (100%), while the maximum pressure was set to 11.3 bar and the RAMP time to 20 min. The reaction tubes (100 mL Teflon PFA vessels) were cooled in an ice bath after the end of the reaction time. Samples were filtered and washed with 20 mL of distilled water to separate the liquefied products from the solid residue. Then, the liquefied products were neutralized by adding NaOH solution. The residue was vacuum-dried overnight at 25 °C and weighed in order to extract the liquefaction efficiency (LE) from the solid residue (eq eq 1).

$$\mathrm{LE}\ (\%) = \frac{\text{Original cellulose (g)} - \text{Residue (g)}}{\text{Original cellulose (g)}} \times 100\% \qquad \text{(eq 1)}$$

The amount of cellulose in the starting materials (original cellulose) was estimated from thermogravimetric analysis (TGA) results (Figure S2, Supporting Information). According to TGA, the cellulose content of BT, WT, and WP was 95, 95, and 76 wt %, respectively.

Characterization. Fourier transform infrared (FTIR) spectra of the samples were recorded on a PerkinElmer Spectrum 2000 spectrometer (PerkinElmer Instrument) with 16 scans at a resolution of 4 cm^{-1}. ^{1}H NMR (400.13 MHz) and ^{13}C NMR (100.62 MHz) analyses were performed on a Bruker Advance 400 spectrometer at 298 K. For each sample, approximately 20 mg (^{1}H NMR) or 120 mg (^{13}C NMR) of the vacuum-dried liquefied cellulose was dissolved in 1 mL of D_2O.

Mettler-Toledo TGA/SDTA 851e was used for the TGA analyses. A total of 3−4 mg of each sample was placed into a 70 μL alumina cup. The samples were then heated at a rate of 10 °C/min from 30 to 550 °C with an O_2 flow rate of 80 mL/min.

A Bruker UltraFlex time-of-flight mass spectrometer with a SCOUT-MTP ion source (Bruker Daltonics, Bremen, Germany) in reflector mode equipped with a nitrogen laser (337 nm) was used for the laser desorption ionization-mass spectrometry (LDI-MS) analysis of the liquefied products. The acceleration voltage was 25 kV and the reflector voltage 26.3 kV. All experiments were run in positive ion mode. A spot of 0.5 μL of the neutralized sample medium was directly applied on the stainless steel plate and allowed to evaporate before analysis. The spectrum obtained for each sample is an accumulation of 1000 laser shots at different spots. The mass-to-charge (m/z) ratio was scanned from 60 to 2000 m/z.

XRD analysis of the solid samples before and after reaction were recorded on PANalytical XPert Pro with CuKR radiation (λ = 0.1541 nm) at 25 °C using a silicon monocrystal sample holder. The intensity (Miller indices) as a function of 2θ was measured, while the angle range was 5−40° and the step was 0.017°. Segal method[43] was used to obtain the crystallinity index (CI) of cellulosic biomasses by applying the height of the I_{200} (characterizes both crystalline and amorphous material, 2θ = 22.7°) and I_{am} (minimum between the peaks at (200) and (110) represents only amorphous material ∼18°) shown in eq eq 2

$$\mathrm{CI} = \frac{I_{200} - I_{am}}{I_{200}} \times 100 \qquad \text{(eq 2)}$$

Scherrer equation[44] was used to obtain average thickness of the cellulose crystallites (D) by measuring the full width at half-maximum (fwhm) of the θ_{max} (200) peak shown in eq eq 3:

$$D\ (\mathrm{nm}) = \frac{K\lambda}{\Delta 2\theta \cos\theta} \qquad \text{(eq 3)}$$

where $\Delta 2\theta$ is the fwhm, θ max is maximum point in radians, K is Scherrer constant (0.94), and λ is the X-ray wavelength (λ = 0.1541 nm).

RESULTS AND DISCUSSION

A process for chemical recycling of waste paper to value-added platform chemicals and carbon nanospheres was developed by utilizing the exceptional combined effect of microwave irradiation and dilute acidic medium. In addition, the effect of different pretreatments on the liquefaction yields was evaluated.

Evaluation of Pretreatment Methods. Different combinations of physical processes (e.g., high temperature, swelling, and sonication) and chemical methods (e.g., acids, bases, and

Table 1. Effect of Different Pretreatments on Microwave-Assisted Liquefaction Efficiency for BT Samples

sample[a]	sonication (min)/ temperature (°C)	residues (g)	liquefaction efficiency (%)[b]
no pretreatment	0	0.263	49.8
acid wetting	0	0.275	47.4
sonication	30/45	0.279	46.5
water swelling	0	0.110	82.0
soda pretreatment	0	0.125	78.9

[a]Sample weight = 0.5 g, RAMP time = 20 min, microwave temperature = 140 °C, holding time (min) = 120, and catalyst concentration = 0.01 g/mL. [b]Liquefaction efficiency for cellulose was calculated based on the TGA estimation of the original cellulose content in BT samples (95 wt %).

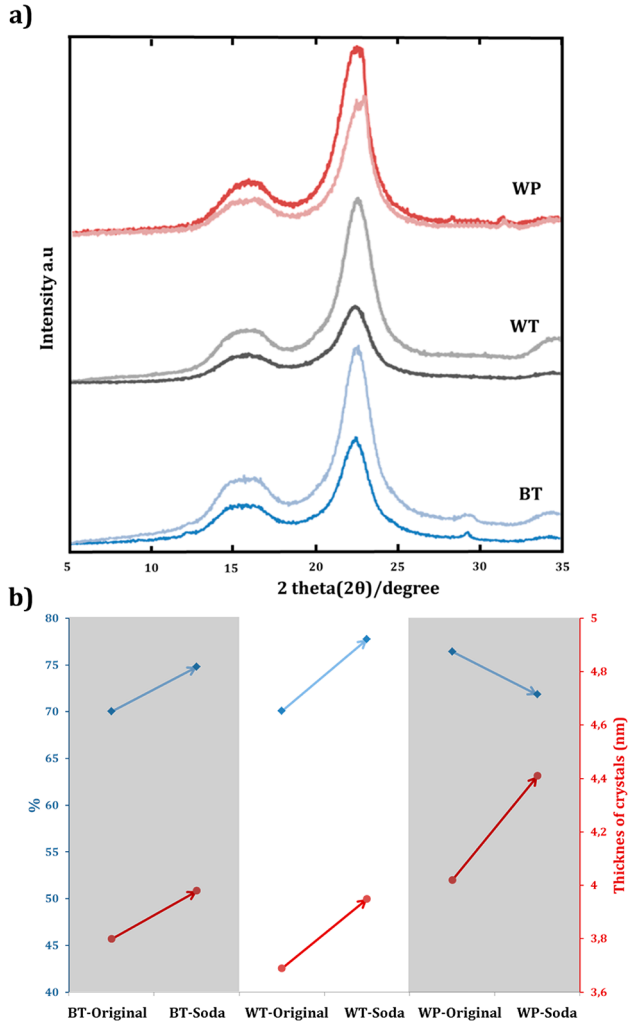

Figure 1. (a) XRD of the different samples before (dark colors) and after (light colors) soda pretreatment. (b) Crystallinity index (CI, blue square) and crystal thickness (*D*, red circle) before and after soda pretreatment.

pure water) were tested on brown paper tissue (BT) samples to find a pretreatment that leads to highest liquefaction efficiency. The microwave reaction conditions were extracted from our previous study on hydrothermal degradation of α-cellulose.[38]

As demonstrated in Table 1, water swelling and soda pretreatments resulted in higher liquefaction efficiencies in comparison to the other proposed pretreatments. Interestingly, short time acid wetting and sonication did not improve the hydrolytic availability of cellulose in the waste paper samples. The increased order of the chains due to shearing and cavitation crystallization of amorphous areas induced by sonication could be a possible reason for this observation.[45]

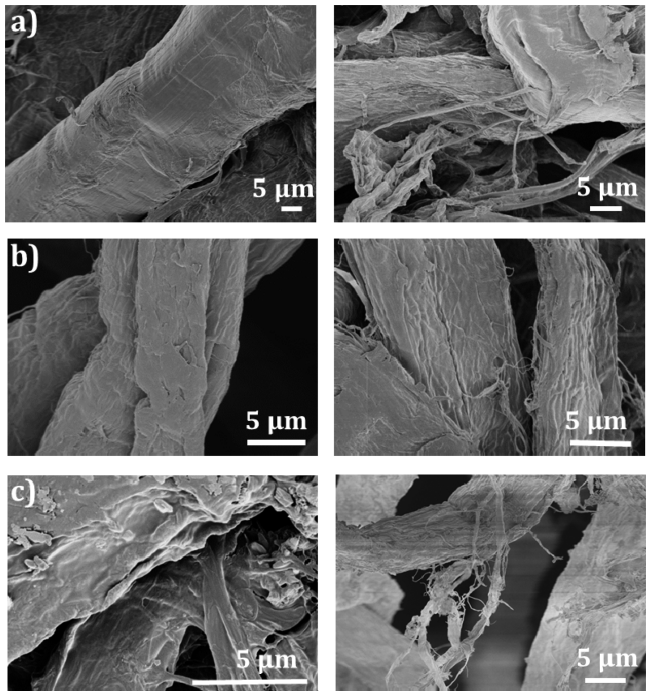

Figure 2. SEM images of (a) BT, (b) WT, and (c) WP before (left) and after (right) soda treatment.

After the initial screening of the pretreatment processes on the BT samples, the impact of the soda pretreatment on the structure of all three waste paper samples, BT, WT, and WP, was studied in more detail. The functional groups on the surface of the samples before and after soda pretreatments were investigated by FTIR (Figure S1, Supporting Information). It was shown that the chemical nature of the cellulosic chains did not change through the procedure, and the chemical state of the materials was preserved. The crystallinity indexes (CI) of the samples after soda pretreatment in Figure 1a and b show two trends depending on the type of sample: (1) An increase in CI was observed for BT and WT probably due to the depolymerization of the amorphous parts, which is supported by weight loss observed during pretreatment (Table S1, Supporting Information). (2) A decrease in CI was observed in the case of WP. This is explained by more dominant decrystallization during the treatment, leading to less depolymerization and higher pulping yield (Table S1, Supporting Information). However, in the same regime, the crystal thickness of the cellulose after soda treatment increased (Figure 1b).

TGA studies (Figure S2, Supporting Information) indicated no significant increase in the cellulose content after soda pretreatment. The remaining large residue in the case of WP samples probably mainly consists of mineral fillers. The pulping efficiency of the soda pretreatment was also evaluated with help of SEM micrographs. The morphological changes in the cellulose fibers are obvious after the pretreatment (Figure 2). The fibers exhibited more disintegrated microfibrils after the alkaline treatment. It seems that heating under alkaline conditions successfully swelled the fibers, dislocated the hydrogen bonds

dx.doi.org/10.1021/sc500686j | ACS Sustainable Chem. Eng. 2015, 3, 177−185

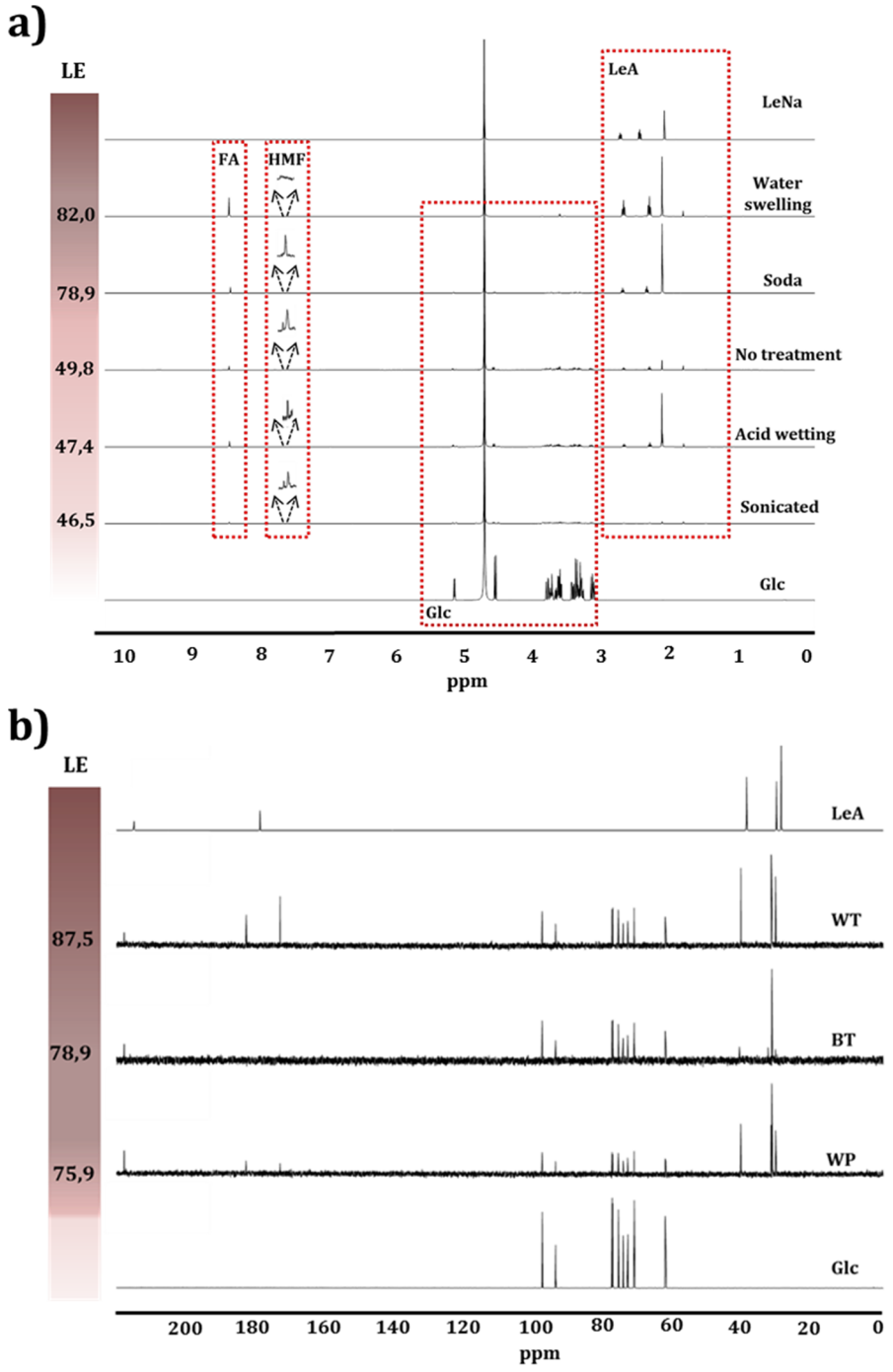

Figure 3. (a) ^{1}H NMR spectra of BT liquefaction products after different pretreatments. (b) ^{13}C NMR spectra of liquefaction products of the different soda-pretreated samples. In addition, the reference spectra for pure levulinic acid as sodium salt (sodium levulinate (LeNa) pH ∼ 7) and glucose are shown. The cellulose LE values are exhibited in the gradient bar.

between the cellulose microfibrils and increased the surface area and porosity, which is expected to facilitate the following acid-catalyzed hydrolysis.

Microwave-Assisted Hydrolysis of Pretreated Waste Papers. Soda and water swelling, the pretreatments that resulted in best liquefaction efficiencies for BT, were applied to the other waste paper samples (WT and WP) before acid-catalyzed microwave-assisted hydrothermal degradation. The obtained liquefaction efficiencies (calculated from remaining weight of the solid residues) were all higher than 69% (Figure 3 and Figure S3, Supporting InformationI).

Qualitative Analysis of the Liquefaction Products. The hydrothermal degradation of the paper samples to small hydrophilic molecules was investigated by ^{1}H and ^{13}C NMR and LDI-MS techniques to identify the final depolymerization degradation products of the cellulose hydrolysis. On the basis of the NMR investigation, the main small molecules formed included glucose (Glc), hydroxymethylfurfural (HMF), levulinic acid (LeA), and formic acid (FA) (Figure 3, Figures S4−S10, Supporting Information).

As was illustrated before for pure α-cellulose,[38] the small molecules formed included products of initial depolymerization

dx.doi.org/10.1021/sc500686j | ACS Sustainable Chem. Eng. 2015, 3, 177−185

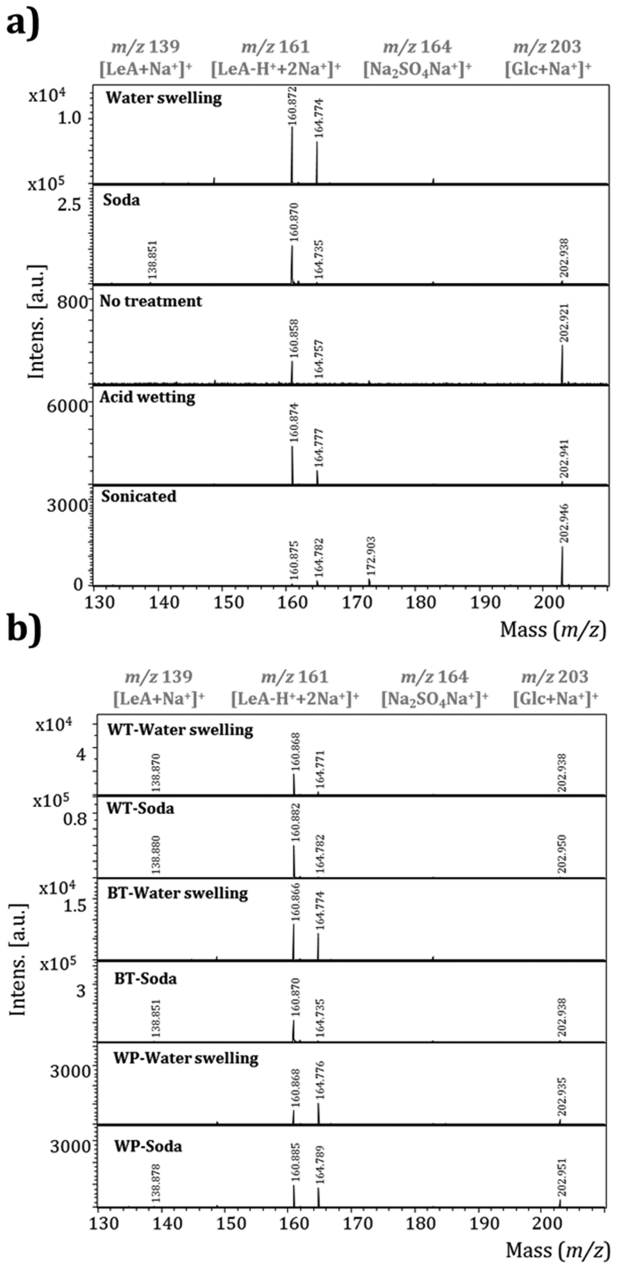

Figure 4. LDI-MS fingerprints of the liquefaction products for the different waste papers and after different pretreatments.

(D-Glc), secondary aqueous phase dehydration products (HMF), and further hydrothermal decomposition products (LeA and FA). In the case of α-cellulose, glucose was the dominating degradation product at lower liquefaction yields, while LeA and FA dominated at higher liquefaction yields. The correlated presentation of the LEs and the spectral patterns of the liquefied products in Figure 3 indicate a similar trend. However, this trend was also clearly affected by the type of pretreatment and type of waste paper.

The obtained chemicals were further fingerprinted by matrix-free LDI-MS in Figure 4 based on our earlier method.[38] The analysis clearly confirmed the NMR identification of the products. The main degradation products observed are denoted in the upper side of the spectra in Figure 4. The analysis of the water-soluble products after different pretreatments is displayed as a function of liquefaction efficiencies. Depending on the conditions used, either glucose or levulinic acid was the dominant water-soluble degradation product. Water swelling and soda treatment increased the amount of levulinic acid $[LeA+Na^+]^+$ and the salt sodium levulinate $[LeA\text{-}H^+ + 2Na^+]^+$. However, all the soda-treated samples demonstrated significantly higher amounts of levulinic acid based on the signal-to-noise values and peak intensities in the mass spectra, indicating that this pretreatment favored levulinic acid formation. All the product mixtures contained levulinic acid with the exception of the sonicated samples, in which glucose $[Glc+Na^+]^+$ dominated. This is in accordance with the low liquefaction yields obtained after this pretreatment. The only sample where glucose was not detected was BT water swelling. As observed in the SEM micrographs, the alkaline treatment increased the surface area and porosity of the microfibrils, facilitating and increasing the rate of depolymerization. This probably resulted in faster depolymerization to glucose and gave more time for further degradation to levulinic acid. The peak at m/z 164.7 corresponds to the formed $[Na_2SO_4Na^+]^+$ salt after neutralization of H_2SO_4 with NaOH.

Selectivity of the Reaction toward Specific Chemicals. A semi-quantitative ^{1}H NMR study of the water-soluble product mixtures was conducted (Figure 5) based on the integrals of all organic compounds present in the liquid phase in order to evaluate the selectivity of the reaction. All the pretreated samples with LE over 69% had faced further reactions of the primary depolymerization product glucose including dehydration (producing HMF), decomposition (producing LeA and FA), and polymerization (producing carbonized-precipitated nanoparticles), although the degree of further reactions was different depending on the starting waste paper characteristics and the pretreatment. Therefore, the pretreatment can be chosen to reach the desired end-products in high yield. For example, for BT with lowest initial CI, water swelling pretreatment exhibited much better selectivity over the final degradation products, producing LeA and FA at ~99% selectivity with respect to the water-soluble product mixtures. At the same time, the original cellulose structure was completely degraded, and solid carbon nanosphere residues were formed (Figures 6 and 7). The best selectivity for the production of Glc was obtained in the case of WP—water swelling with water-soluble products consisting of ~83% of Glc.

Figure 5 shows that the selectivity over the final products was enhanced by the water swelling pretreatment. The LE values were generally in the same regime. The largest difference was observed between soda-treated and water-swelled WT samples, where the soda pretreatment resulted in 18% higher LE. This observation can be correlated to the more fibrous morphology of WT and increased disintegration of microfibrils enhancing the hydrolysis rate. This morphological difference is also illustrated by the SEM images in Figure 2. A small amount of HMF, an intermediate of glucose degradation, was detected in all samples. The low amount of HMF observed confirms its intermediate nature and low stability under the applied conditions, as well as the efficiency of the subsequent dehydration—polymerization process to LeA, FA and CN.

Qualitative Study of Solid Residues. The dark black visual feature of the obtained solid residues indicated the presence of carbonous structures (Figure S11, Supporting Information). These solid residues were further investigated by FTIR, XRD, and SEM analyses. The characterization of the functional groups in the remaining solid residue revealed the presence of carbonous structures and in some cases the coexistence of

dx.doi.org/10.1021/sc500686j | ACS Sustainable Chem. Eng. 2015, 3, 177−185

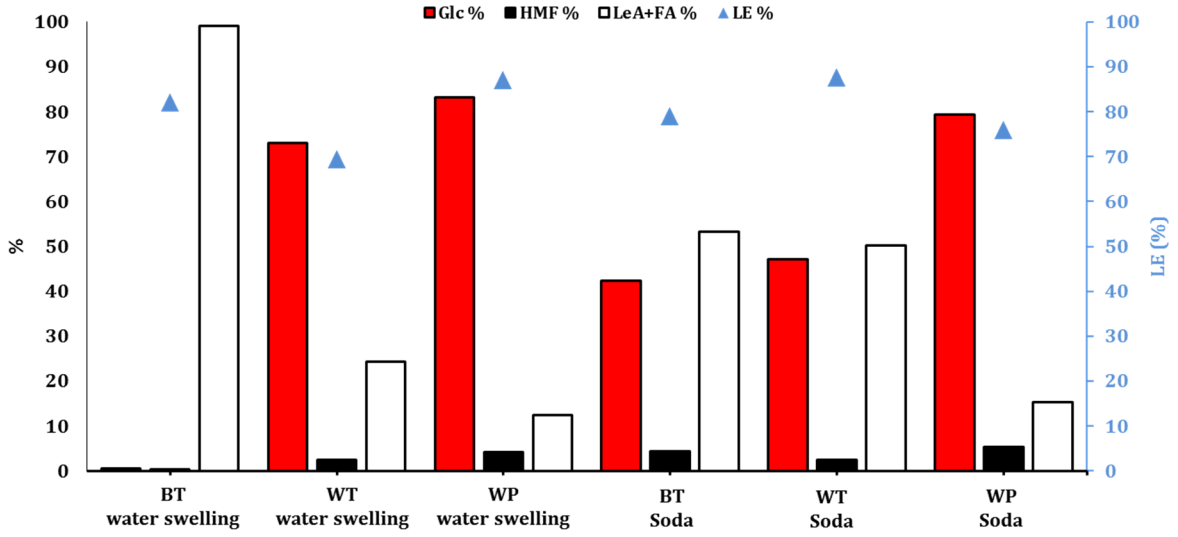

Figure 5. Liquefaction yield and molar composition of the liquefied fraction extracted from ^{1}H NMR analysis.

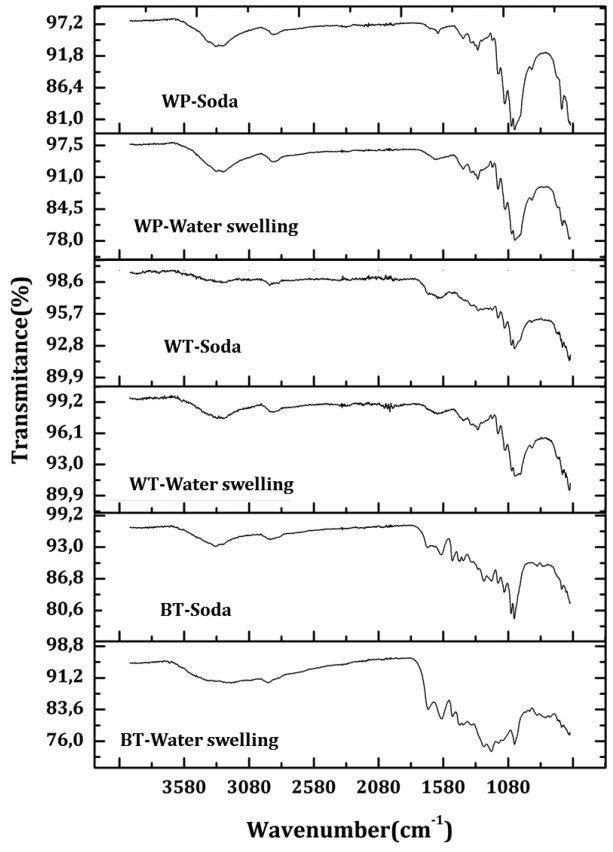

Figure 6. FTIR spectra of the solid residues from the microwave-assisted degradation after different pretreatments.

unreacted cellulose. FTIR spectra of the residues after microwave depolymerization−degradation reactions (Figure 6) proved changes in functional groups in comparison to pure cellulose at three areas: (1) O−H stretching at 3200 cm^{-1} combined with alkyl C−H stretching, alkenyl C−H stretching with alcohol O−H stretching, or/and carboxylic acid O−H stretching, (2) aromatic C═C and C═O stretching at 1500−1750 cm^{-1}, and (3) C−O stretching peaks in the region 1000−1260 cm^{-1}.

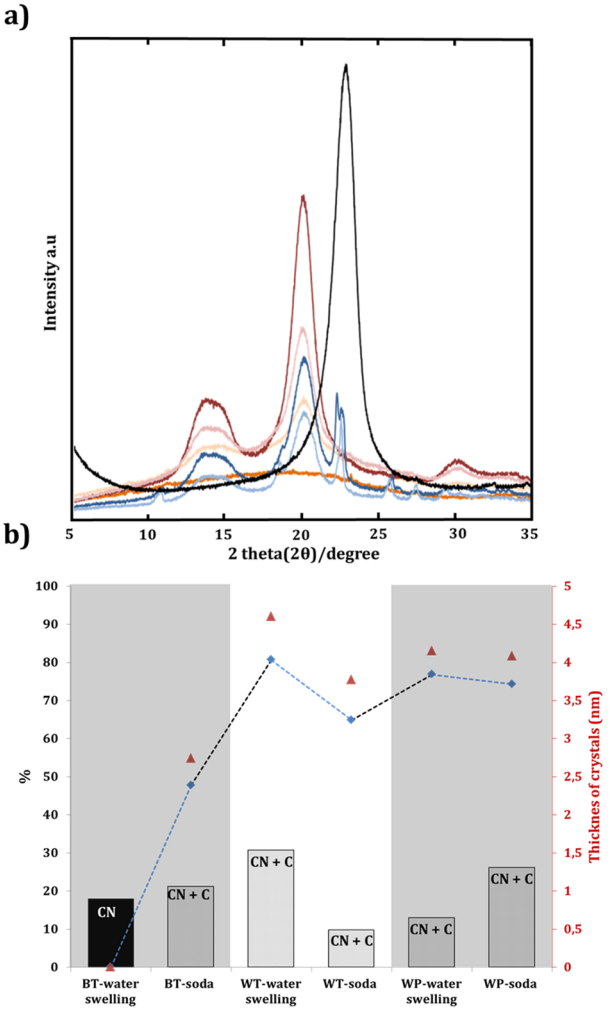

Figure 7. (a) X-ray diffraction patterns of the solid residues from microwave-assisted degradation of BT−soda (light orange), BT−water swelling (dark orange), WT−soda (light purple), WT−water swelling (dark purple), WP−soda (light blue), and WP−water swelling (dark blue). Graphitized carbon black is shown as a reference (black). (b) the correlation curves for the crystallinity index (CI, blue squares) and crystal thickness (*D*, red triangles) of the remaining cellulose (C). The bars illustrate the wt % of cellulose (C) and solid carbon nanosphere (CN) residues.

dx.doi.org/10.1021/sc500686j | *ACS Sustainable Chem. Eng.* 2015, 3, 177−185

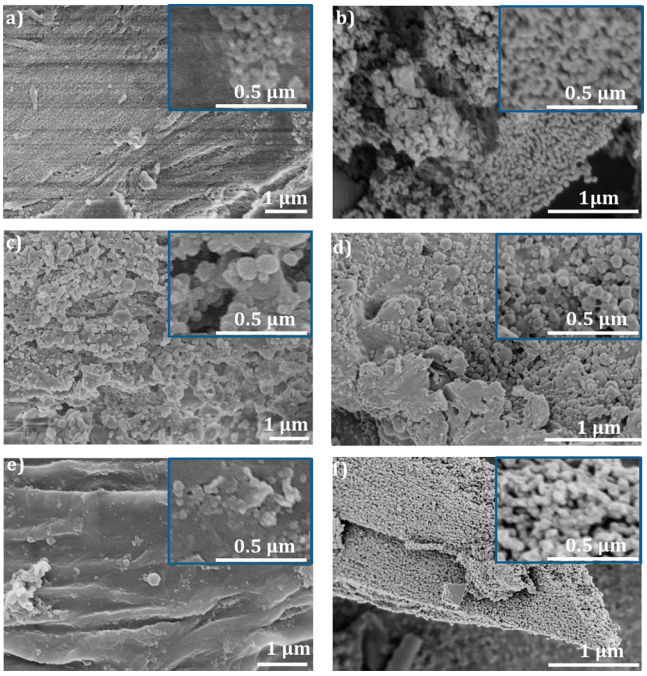

Figure 8. Typical SEM images of the residues of (a) BT−soda, (b) BT−water swelling, (c) WT−soda, (d) WT−water swelling, (e) WP−soda, and (f) WP−water swelling samples.

The X-ray diffraction patterns of the solid residues from the BT samples after different pretreatments are displayed in Figure S12 of the Supporting Information. The diffraction patterns were combinations of typical cellulose peaks ((110) $2\theta \sim 15.5°$ and (200) and $2\theta \sim 22.7°$) and amorphous carbon structures (with small graphitized region diffraction peak for BT−water swelling and BT−soda on $2\theta \sim 26.3°$). Only in the case of the BT−water swelling sample, all the original cellulose had degraded, and no diffraction peaks of cellulose were observed. Instead, almost pure carbonous structures were observed. In agreement with the NMR results, it thus seems that cellulose was entirely depolymerized to glucose followed by complete further conversion of glucose forming LeA, FA, and solid carbon nanospheres. In all the other cases, the coexistence of unreacted cellulose and precipitated carbonized structures is observed with varying degree of carbonization−graphitization and varying degree of crystallinity for the remaining cellulose (Figure 7). Similar spherical carbon particles produced during traditional hydrothermal degradation of biomass have received growing attention due to their sophisticated properties such as low density, high surface area, electronic properties, high thermal stability, and biocompatibility.[46] From these properties, a variety of potential applications including catalyst supports, column packing materials, lubricating materials, materials for electrical-optical devices, and biomedical application can be anticipated.[41,47−49]

Scheme 1. Schematic Presentation of Microwave-Assisted Reaction Process and Its Different Stages

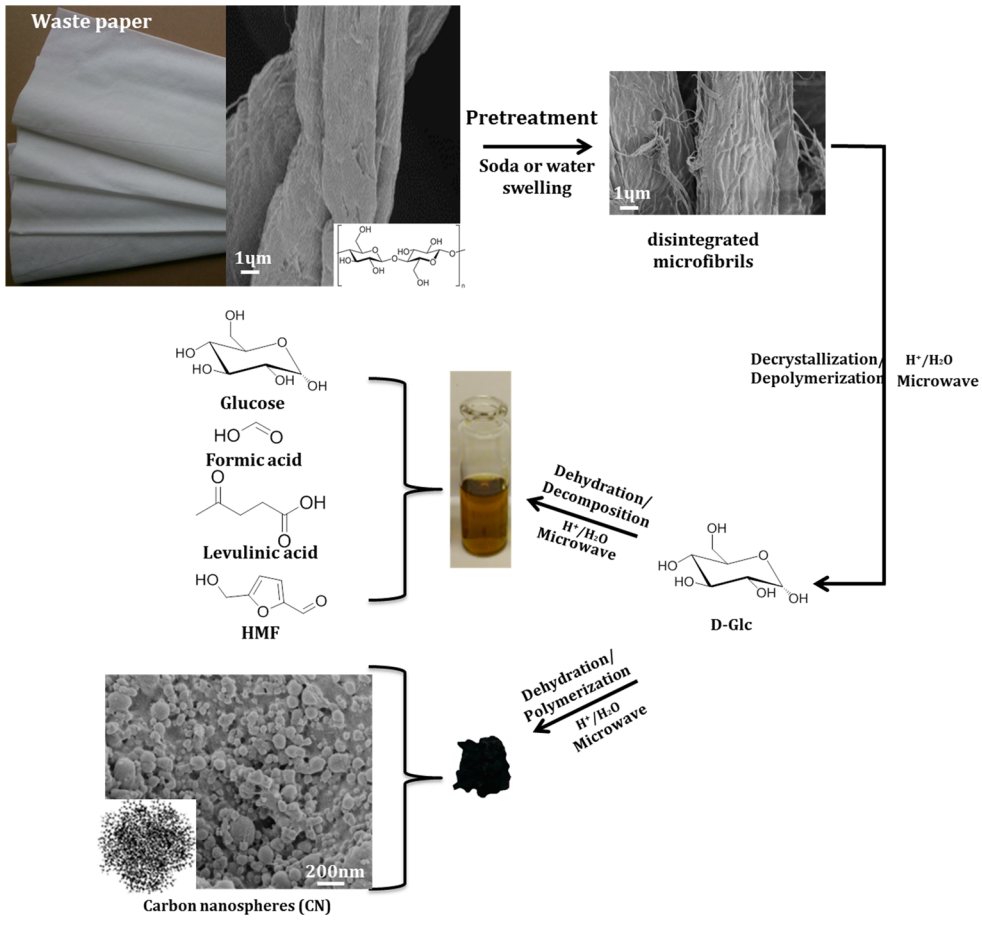

dx.doi.org/10.1021/sc500686j | ACS Sustainable Chem. Eng. 2015, 3, 177−185

The morphological changes caused by microwave-assisted degradation of water swelled- and soda-pretreated samples were evaluated by SEM. In consistency with the FTIR and XRD results, fine nanometric spherical carbon structures were visible in all the samples. The morphological transformation from native fibrous cellulose to the polymerized-precipitated carbon nanospheres was complete in the case of BT−water swelling (Figure 8a) with no signs of any remaining fibrous structures. The remaining cellulose fibers were, however, visible when the liquefaction yield was lower (see WP−soda and WT−water swelling in Figure 8c and f, respectively).

The whole microwave-assisted waste paper recycling process and its different stages are summarized in Scheme 1. Mixtures with different compositions of Glc, HMF, LeA, FA, and solid carbonized particles were obtained at the end of the reaction with the exception of the most degraded sample, BT−water swelling, which realized completely with chemo-selective production of LeA and FA together with some precipitated carbon nanospheres.

CONCLUSIONS

A microwave-assisted process was developed for recycling waste paper to functional chemicals and carbon nanospheres. The dilute acidic conditions and microwave irradiation in combination with pretreatments, like water swelling and soda treatment, resulted in exceptionally high liquefaction efficiencies. The liquefaction yields demonstrated that soda and water swelling pretreatments successfully swelled the cellulosic fibers, increasing the surface area and disintegrating the microfibrils making them more susceptible to microwave-assisted degradation. Liquefaction efficiencies as high as 88 wt % of the original cellulose in waste paper were achieved. The reaction was chemo-selective resulting in a few well-defined products. At lower liquefaction yields, glucose was the dominating degradation product. At higher liquefaction yields, glucose was dehydrated to HMF, which was rapidly further converted to levulinic acid and formic acid and/or polymerized to solid carbon nanospheres. The degradation product composition was also influenced by the type of pretreatment and type of waste paper. The selectivity of the reaction could reach up to ∼99% of LeA and FA in the liquid phase, while Glc could be produced at 83% selectivity. The developed process displays significant potential for future production of platform chemicals from waste paper as even low quality paper waste not suitable for traditional recycling can be turned to value-added products.

ASSOCIATED CONTENT

Supporting Information

More studies and characterizations on the materials using FTIR, TGA, NMR (^{1}H and ^{13}C), and XRD techniques. This material is available free of charge via the Internet at http://pubs.acs.org.

AUTHOR INFORMATION

Corresponding Author

*E-mail: minna@kth.se. Phone +46-087908271.

Notes

The authors declare no competing financial interest.

ACKNOWLEDGMENTS

The Swedish Research Council (VR) is acknowledged for financial support (Contract Grant 2012-4369).

ABBREVIATIONS

BT, brown paper tissues; WT, white paper tissues; WP, white printing paper; SA, sulfuric acid; LE, liquefaction efficiency; LDI-MS, laser desorption ionization-mass spectrometry; CI, crystallinity index; Glc, glucose; HMF, hydroxymethylfurfural; LeA, levulinic acid; FA, formic acid; LeNa, sodium levulinate; CN, carbon nanospheres; C, cellulose

REFERENCES

(1) Pu, Y.; Hu, F.; Huang, F.; Davison, B.; Ragauskas, A. Assessing the molecular structure basis for biomass recalcitrance during dilute acid and hydrothermal pretreatments. *Biotechnol. Biofuels* **2013**, *6* (1), 15.

(2) Rinaldi, R.; Schüth, F. Acid hydrolysis of cellulose as the entry point into biorefinery schemes. *ChemSusChem* **2009**, *2* (12), 1096−1107.

(3) General Overview of What's in America's Trash. U.S. Environmental Protection Agency. http://www.epa.gov/osw/wycd/catbook/what.htm (accessed December 2014).

(4) Rahman, M. O.; Hussain, A.; Basri, H. A critical review on waste paper sorting techniques. *Int. J. Environ. Sci. Technol.* **2014**, *11* (2), 551−564.

(5) Monte, M. C.; Fuente, E.; Blanco, A.; Negro, C. Waste management from pulp and paper production in the European Union. *Waste Manage.* **2009**, *29* (1), 293−308.

(6) Yang, W.; Sen, A. One-step catalytic transformation of carbohydrates and cellulosic biomass to 2,5-dimethyltetrahydrofuran for liquid fuels. *ChemSusChem* **2010**, *3* (5), 597−603.

(7) Tang, Z.; Deng, W.; Wang, Y.; Zhu, E.; Wan, X.; Zhang, Q.; Wang, Y. Transformation of cellulose and its derived carbohydrates into formic and lactic acids catalyzed by vanadyl cations. *ChemSusChem* **2014**, *7* (6), 1557−1567.

(8) *Renewable Biological Systems for Alternative Sustainable Energy Production*; Agricultural Services Bulletin 128; Miyamoto, K., Ed.; Food and Agriculture Organization of the United Nations (FAO): Rome, 1997.

(9) Converting Waste Agricultural Biomass into a Resource. United Nations Environment Programme. http://www.unep.org/ietc/Portals/136/Publications/Waste%20Management/WasteAgriculturalBiomassEST_Compendium.pdf (accessed December 2014).

(10) Chundawat, S. P. S.; Bellesia, G.; Uppugundla, N.; da Costa Sousa, L.; Gao, D.; Cheh, A. M.; Agarwal, U. P.; Bianchetti, C. M.; Phillips, G. N.; Langan, P.; Balan, V.; Gnanakaran, S.; Dale, B. E. Restructuring the crystalline cellulose hydrogen bond network enhances its depolymerization rate. *J. Am. Chem. Soc.* **2011**, *133* (29), 11163−11174.

(11) Zugenmaier, P. Conformation and packing of various crystalline cellulose fibers. *Prog. Polym. Sci.* **2001**, *26* (9), 1341−1417.

(12) Gardner, K. H.; Blackwell, J. The structure of native cellulose. *Biopolymers* **1974**, *13* (10), 1975−2001.

(13) Takahashi, Y.; Matsunaga, H. Crystal structure of native cellulose. *Macromolecules* **1991**, *24* (13), 3968−3969.

(14) Lim, J. S.; Abdul Manan, Z.; Wan Alwi, S. R.; Hashim, H. A review on utilisation of biomass from rice industry as a source of renewable energy. *Renewable Sustainable Energy Rev.* **2012**, *16* (5), 3084−3094.

(15) Sun, Y.; Cheng, J. Hydrolysis of lignocellulosic materials for ethanol production: a review. *Bioresour. Technol.* **2002**, *83* (1), 1−11.

(16) Pang, Y. Z.; Liu, Y. P.; Li, X. J.; Wang, K. S.; Yuan, H. R. Improving biodegradability and biogas production of corn stover through sodium hydroxide solid state pretreatment. *Energy Fuels* **2008**, *22* (4), 2761−2766.

(17) Gabhane, J.; Prince William, S. P. M.; Vaidya, A. N.; Mahapatra, K.; Chakrabarti, T. Influence of heating source on the efficacy of lignocellulosic pretreatment − A cellulosic ethanol perspective. *Biomass Bioenergy* **2011**, *35* (1), 96−102.

(18) Lee, J. S.; Parameswaran, B.; Lee, J. P.; Park, S. C. Recent developments of key technologies on cellulosic ethanol production. *J. Sci. Ind. Res.* **2008**, *67* (11), 865−873.

(19) Li, Y.; Ruan, R.; Chen, P. L.; Liu, Z.; Pan, X.; Lin, X.; Liu, Y.; Mok, C. K.; Yang, T. Enzymatic hydrolysis of corn stover pretreated by

combined dilute alkaline treatment and homogenization. *Trans. Am. Soc. Agric. Eng.* **2004**, *47* (3), 821−825.
(20) Lee, J.-W.; Jeffries, T. W. Efficiencies of acid catalysts in the hydrolysis of lignocellulosic biomass over a range of combined severity factors. *Bioresour. Technol.* **2011**, *102* (10), 5884−5890.
(21) Bensah, E. C.; Mensah, M. Chemical pretreatment methods for the production of cellulosic ethanol: Technologies and innovations. *Int. J. Chem. Eng.* **2013**, *2013*, 21.
(22) Yang, X.; Odelius, K.; Hakkarainen, M. Microwave-assisted reaction in green solvents recycles PHB to functional chemicals. *ACS Sustainable Chem. Eng.* **2014**, *2* (9), 2198−2203.
(23) Wu, D.; Hakkarainen, M. A closed-loop process from microwave-assisted hydrothermal degradation of starch to utilization of the obtained degradation products as starch plasticizers. *ACS Sustainable Chem. Eng.* **2014**, *2* (9), 2172−2181.
(24) Ludlow-Palafox, C.; Chase, H. A. Microwave-induced pyrolysis of plastic wastes. *Ind. Eng. Chem. Res.* **2001**, *40* (22), 4749−4756.
(25) Tsintzou, G.; Achilias, D. Chemical recycling of polycarbonate based wastes using alkaline hydrolysis under microwave irradiation. *Waste Biomass Valor.* **2013**, *4* (1), 3−7.
(26) Centi, G.; Perathoner, S. Opportunities and prospects in the chemical recycling of carbon dioxide to fuels. *Catal. Today* **2009**, *148* (3−4), 191−205.
(27) Van de Vyver, S.; Geboers, J.; Jacobs, P. A.; Sels, B. F. Recent advances in the catalytic conversion of cellulose. *ChemCatChem.* **2011**, *3* (1), 82−94.
(28) Luque, R.; Clark, J. H. Biodiesel-like biofuels from simultaneous transesterification/esterification of waste oils with a biomass-derived solid acid catalyst. *ChemCatChem.* **2011**, *3* (3), 594−597.
(29) Qi, X.; Watanabe, M.; Aida, T. M.; Smith, R. L. Fast transformation of glucose and di-/polysaccharides into 5-hydroxymethylfurfural by microwave heating in an ionic liquid/catalyst system. *ChemSusChem* **2010**, *3* (9), 1071−1077.
(30) Balu, A. M.; Budarin, V.; Shuttleworth, P. S.; Pfaltzgraff, L. A.; Waldron, K.; Luque, R.; Clark, J. H. Valorisation of orange peel residues: Waste to biochemicals and nanoporous materials. *ChemSusChem* **2012**, *5* (9), 1694−1697.
(31) Dutta, A.; Gupta, D.; Patra, A. K.; Saha, B.; Bhaumik, A. Synthesis of 5-hydroxymethylfurural from carbohydrates using large-pore mesoporous tin phosphate. *ChemSusChem* **2014**, *7* (3), 925−933.
(32) Crépy, L.; Chaveriat, L.; Banoub, J.; Martin, P.; Joly, N. Synthesis of cellulose fatty esters as plastics—influence of the degree of substitution and the fatty chain length on mechanical properties. *ChemSusChem* **2009**, *2* (2), 165−170.
(33) De, S.; Dutta, S.; Saha, B. One-pot conversions of lignocellulosic and algal biomass into liquid fuels. *ChemSusChem* **2012**, *5* (9), 1826−1833.
(34) Pollastri, M. P.; Devine, W. G. Microwave Synthesis. In *Green Techniques for Organic Synthesis and Medicinal Chemistry*; John Wiley & Sons, Ltd: New York, 2012; pp 325−342.
(35) de la Hoz, A.; Diaz-Ortiz, A.; Moreno, A. Microwaves in organic synthesis. Thermal and non-thermal microwave effects. *Chem. Soc. Rev.* **2005**, *34* (2), 164−178.
(36) Fan, J.; De bruyn, M.; Budarin, V. L.; Gronnow, M. J.; Shuttleworth, P. S.; Breeden, S.; Macquarrie, D. J.; Clark, J. H. Direct microwave-assisted hydrothermal depolymerization of cellulose. *J. Am. Chem. Soc.* **2013**, *135* (32), 11728−11731.
(37) Möller, M.; Harnisch, F.; Schroder, U. Hydrothermal liquefaction of cellulose in subcritical water-the role of crystallinity on the cellulose reactivity. *RSC Adv.* **2013**, *3* (27), 11035−11044.
(38) Hassanzadeh, S.; Aminlashgari, N.; Hakkarainen, M. Chemo-selective high yield microwave assisted reaction turns cellulose to green chemicals. *Carbohydr. Polym.* **2014**, *112* (0), 448−457.
(39) Cherubini, F. The biorefinery concept: Using biomass instead of oil for producing energy and chemicals. *Energy. Conver. Manage.* **2010**, *51* (7), 1412−1421.
(40) Zheng, G.; Lee, S. W.; Liang, Z.; Lee, H.-W.; Yan, K.; Yao, H.; Wang, H.; Li, W.; Chu, S.; Cui, Y. Interconnected hollow carbon nanospheres for stable lithium metal anodes. *Nat. Nanotechnol.* **2014**, *9* (8), 618−623.
(41) Jing Wang, Z. H.; Jianxun, X.; Yuliang, Z. Therapeutic applications of low-toxicity spherical nanocarbon materials. *NPG Asia Mater.* **2014**, *6*, e84.
(42) Obumneme O, O. The effect of pulping concentration treatment on the properties of microcrystalline cellulose powder obtained from waste paper. *Carbohydr. Polym.* **2013**, *98* (1), 721−725.
(43) Segal, L.; Creely, J. J.; Martin, A. E.; Conrad, C. M. An empirical method for estimating the degree of crystallinity of native cellulose using the X-ray diffractometer. *Text. Res. J.* **1959**, *29* (10), 786−794.
(44) Scherrer, P. Bestimmung der größe und der inneren struktur von kolloidteilchen mittels röntgenstrahlen. *Nachr. Ges. Wiss. Goettingen, Math.-Phys. Kl.* **1918**, *1918*, 98−100.
(45) Tischer, P. C. S. F.; Sierakowski, M. R.; Westfahl, H.; Tischer, C. A. Nanostructural reorganization of bacterial cellulose by ultrasonic treatment. *Biomacromolecules* **2010**, *11* (5), 1217−1224.
(46) Deshmukh, A. A.; Mhlanga, S. D.; Coville, N. J. Carbon spheres. *Mater. Sci. Eng., R* **2010**, *70* (1−2), 1−28.
(47) Nieto-Marquez, A.; Romero, R.; Romero, A.; Valverde, J. L. Carbon nanospheres: Synthesis, physicochemical properties and applications. *J. Mater. Chem.* **2011**, *21* (6), 1664−1672.
(48) Romero-Anaya, A. J.; Ouzzine, M.; Lillo-Ródenas, M. A.; Linares-Solano, A. Spherical carbons: Synthesis, characterization and activation processes. *Carbon* **2014**, *68* (0), 296−307.
(49) Selvi, B. R.; Jagadeesan, D.; Suma, B. S.; Nagashankar, G.; Arif, M.; Balasubramanyam, K.; Eswaramoorthy, M.; Kundu, T. K. Intrinsically fluorescent carbon nanospheres as a nuclear targeting vector: Delivery of membrane-impermeable molecule to modulate gene expression in vivo. *Nano Lett.* **2008**, *8* (10), 3182−3188.